

 Open access • Journal Article • DOI:10.1002/CRAT.2170310218

Thermodiffusion and morphological stability in convectionless crystal growth systems from melts and melt-solutions — [Source link](#)

Peter Rudolph, Torsten Boeck, P. Schmidt

Institutions: Institut für Kristallzüchtung, Radboud University Nijmegen

Published on: 01 Jan 1996 - Crystal Research and Technology (Akademie verlag gmbh)

Related papers:

- [Observation of NaClLiCl high-temperature phases by gold decoration on the solid—melt interface of czochralski grown crystals](#)
- [Temperature and thickness dependence of electrical and thermal transport coefficients of Bi_{1-x}Sb_x films in an anisotropic, non-degenerate two-band model](#)
- [Electrophysical Properties of GeSexTe_{1-x} Single Crystals Grown by Physical Vapor Transport \(PVT\).](#)
- [A thermodynamic model of The Hg_{0.8} Cd_{0.2} Te-Iodine Transport System. I. Te-saturated source material](#)
- [Chemistry of organic eutectics \(III\). \$\alpha\$ -Naphthol-naphthalene system](#)

Share this paper:    

View more about this paper here: <https://typeset.io/papers/thermodiffusion-and-morphological-stability-in-3krj2zax8d>

PDF hosted at the Radboud Repository of the Radboud University Nijmegen

The following full text is a publisher's version.

For additional information about this publication click this link.

<http://hdl.handle.net/2066/28084>

Please be advised that this information was generated on 2022-05-31 and may be subject to change.

P. RUDOLPH, T. BOECK, P. SCHMIDT

Institut für Kristallzüchtung (IKZ), Berlin, Germany, and
University of Nijmegen, Department of Experimental and Solid State Physics III, NL

Thermodiffusion and Morphological Stability in Convectionless Crystal Growth Systems from Melts and Melt-Solutions

Crystal growth experiments of multicomponent systems under microgravity require an exact analysis of the diffusion phenomena in the nutrient fluid phase. The contribution of the Soret effect to the transport and distribution of matter in a convectionless casting arrangement for shaped crystal growth and in THM melt-solution zones have been investigated. Some semiconductor systems were analysed from experimental ($\text{Bi}_{1-x}\text{Sb}_x$ mixed crystals) and theoretical (PbTe, InP, GaAs, CdTe compounds) point of view. The criterion for constitutional supercooling was correspondingly modified. It has been distinguished between associated (AIV–BVI, AII–BVI) and dissociated (AIII–BV) melt-solutions, containing different species of diffusion (molecules or atoms, respectively).

Kristallzüchtungsexperimente mit mehrkomponentigen Systemen unter Schwerelosigkeit erfordern eine exakte Behandlung der Diffusionsphänomene in der fluiden Nährphase. Es wurde der Beitrag des Soret-Effektes zum Massetransport und zur -verteilung in einer konvektionsfreien Gießanordnung zur Züchtung von Formkristallen und in THM-Schmelzlösungszonen untersucht. Dazu wurden einige Halbleitersysteme experimentell ($\text{Bi}_{1-x}\text{Sb}_x$ Mischkristalle) und theoretisch (PbTe-, InP-, GaAs-, CdTe-Verbindungen) überprüft. Das Kriterium für Konzentrationsunterkühlung wurde entsprechend modifiziert. Es wurde zwischen assoziierten (AIV–BVI, AII–BVI) und dissoziierten (AIII–BV) Schmelzlösungen unterschieden, die unterschiedliche Diffusionsspezies (Moleküle bzw. Atome) aufweisen.

1. Introduction

For an analysis of crystal growth phenomena under conditions of microgravity (μg), the normal freezing of sealed containers (Bridgman growth, shaped crystal growth by casting), the travelling heater method (THM) and the sublimation-condensation, are advantageous methods (FEUERBACHER et al.). A specific temperature profile is chosen in order to control the interface mass transport rates and to supply the latent heat of fusion, in other words, characteristic uniaxial temperature gradients must be engineered (Fig. 1). Therefore, gradients of temperature in the nutrient phases must exist, leading to buoyancy-driven convection in normal ground based experiments. Conversely under μg conditions and the prevention of Maragoni flows, the mass transfer is dominated by diffusion composed of ordinary Fick flow j_{OD} , and thermodiffusive transport j_{TD} . The so called Soret effect (SORET) of thermodiffusion is a cross-effect resulting from the interaction between the thermodynamic fluxes of heat and matter in a mixture of two or more components. Both, heat conduction and diffusion are coupled to transport heat and matter from regions which temperature and concentration are not in equilibrium. Therefore, temperature gradients cause concentration gradients in an initially homogeneous solu-

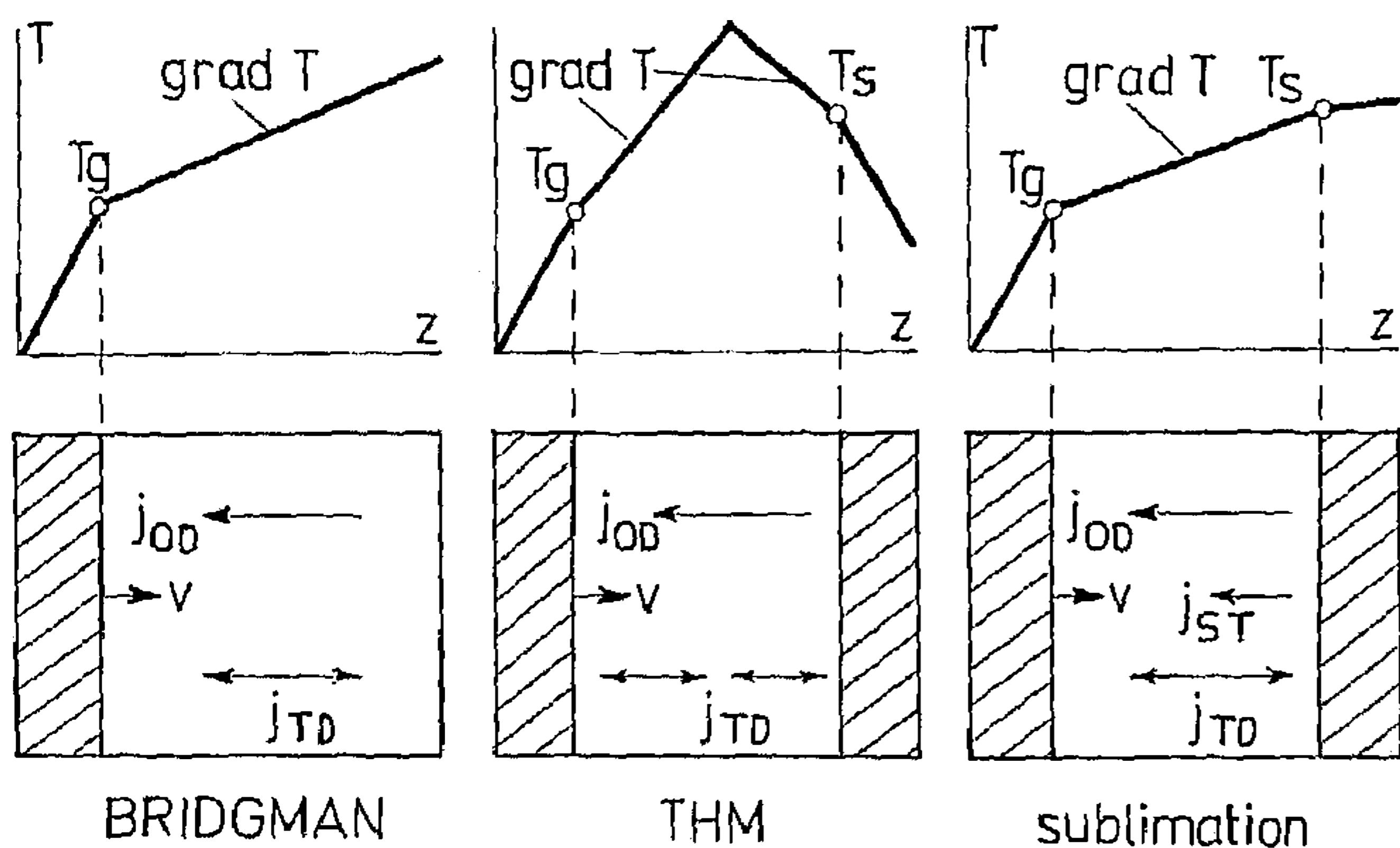


Fig. 1. The principles of diffusion-controlled crystal growth methods usually applied under μg conditions (T - temperature, z - distance, T_G - growth temperature, T_S - solution or sublimation temperature, $\text{grad } T$ - temperature gradient in the fluid phase, v - growth rate, j_{OD} - ordinary diffusion flow, j_{TD} - thermodiffusion flow, j_{ST} - Stefan flow)

tion until the separation of components results in the thermodynamic equilibrium. Thus, the total diffusion flow of the solvent B in a solution is

$$j_B = j_{OD} + j_{TD} = -\rho D \text{grad } c_B + c_A c_B D' \text{grad } T \quad (1)$$

with ρ being the mass density of the melt-solution, D the ordinary diffusion coefficient, c_A and c_B the concentrations of solute A and solvent B in weight fraction, T the absolute temperature and $D' = D_0/c_A c_B = D S_T$ the thermal diffusion coefficient with S_T the Soret coefficient.

To date, the exact values and even the sign of S_T of many material systems is unknown (ROSENBERGER). Current convention assigns a positive value to S_T when the solvent B is found to be the light component and moves to the hot region. Various practical and theoretical methods to determine the value of S_T are described. The most convenient experimental procedure appears to be the shear cell arrangement (NACHTRIEB). We have carried out the rapid quenching of capillary ampoules, which have remained for an extended time at a constant temperature gradient (BOECK; SCHMIDT). According to WINTER and DRICKAMER a value may be predicted from the relation

$$S_T = \frac{m - M}{m c_B + M(1 - c_B)} \Delta E / k T^2 \quad (2)$$

where m , M are the molecular weights of solute and solvent, respectively, ΔE is the activation energy, c_B the concentration of solvent, T the absolute temperature and k the Boltzmann constant.

Particular attention is required for various melt-solutions. It is well known (JORDAN) that a much stronger interaction exists between unlike atoms of the II-VI and IV-VI compounds than of the III-V compounds in the molten state. Therefore, a low degree of dissociation $\beta_1 = 0.05$, i.e., concentration of separate dissimilar atoms in the II-VI and IV-VI melt solutions, will be obtained and gives rise to separate AB molecules (solute) and atomic solvent B involved in the diffusion fluxes. We have used the physicochemical parameters listed in Table 1.

Depending on the total value and sign of the Soret coefficient, the concentration inhomogeneities in the nutrient will be decreased and will influence the critical growth conditions (maximum growth rate) in comparison with conditions resulting from the ordinary diffusion alone. We have investigated the practical contribution of the Soret effect on the segregation function in convectionless Bridgman-grown $\text{Bi}_{1-x}\text{Sb}_x$ mixed

Table 1
Some physicochemical parameters of semiconductor systems

Crystal	Melt (A, B)	Solvent (B)	T [K]	c_B [mass %]	S_T ($\times 10^{-3} \text{ K}^{-1}$)	
					(th)	(exp)
GaAs	Ga, As	Ga	1073	0.9576	+0.2 ¹⁾	
InP	In, P	In	1073	0.9882	-7.5 ¹⁾	
PbTe	PbTe, Te	Te	900	0.3226		+2.0 ²⁾
CdTe	CdTe, Te	Te	1073	0.4437	+1.4	
Bi-Sb	Bi, Sb	Sb	550	0.0020	+2.0 ³⁾	+4.0 ⁴⁾

1) CHEN, MATTES, 2) BOECK, 3) DISMUKES, YIM, 4) SCHMIDT

crystals, and the theoretical distribution of components in THM zones of CdTe:Te, PbTe:Te, GaAs:Ga, and InP:In.

2. Convectionless Bridgman growth in thin moulds

In order to suppress buoyancy- and surface tension-driven convection in melt and melt-solution crystal growth systems at normal gravity (1g), strong axial temperature gradients and as narrow as possible vertical melt columns are desirable. We applied a special Bridgman growth arrangement for $\text{Bi}_{1-x}\text{Sb}_x$ mixed crystals using a micro mould system consisting of parallel optically flat plates made of fused silica (Fig. 2). The ingot chamber for the crystallization process had the dimension 50 mm in length, 5 mm wide and of 1 mm thickness. A linear uniaxial temperature gradient of 15 K cm^{-1} was maintained by a pair of Kanthal meanders.

After the positioning of a cleaved single crystal seed on the bottom of the ingot chamber and the heating of the otherwise empty mould to growth temperature, an externally molten starting charge with a mole fraction $x = 0.025$ was poured through the filling port into the crystallization chamber. The growth process with a crystallization velocity of 0.2 mm h^{-1} was achieved by computer-controlled cooling with a rate of 0.3 K h^{-1} over a period of 300 h. Monocrystalline, elongated thin laminas of high purity and very good structural perfection were obtained (RUDOLPH; SCHMIDT) and the axial concentration distribution were determined by electron probe microanalysis (EPMA). Figure 3 shows the segregation functions of the Sb mole fraction taken from EPMA measurements (CHRIST et al.)

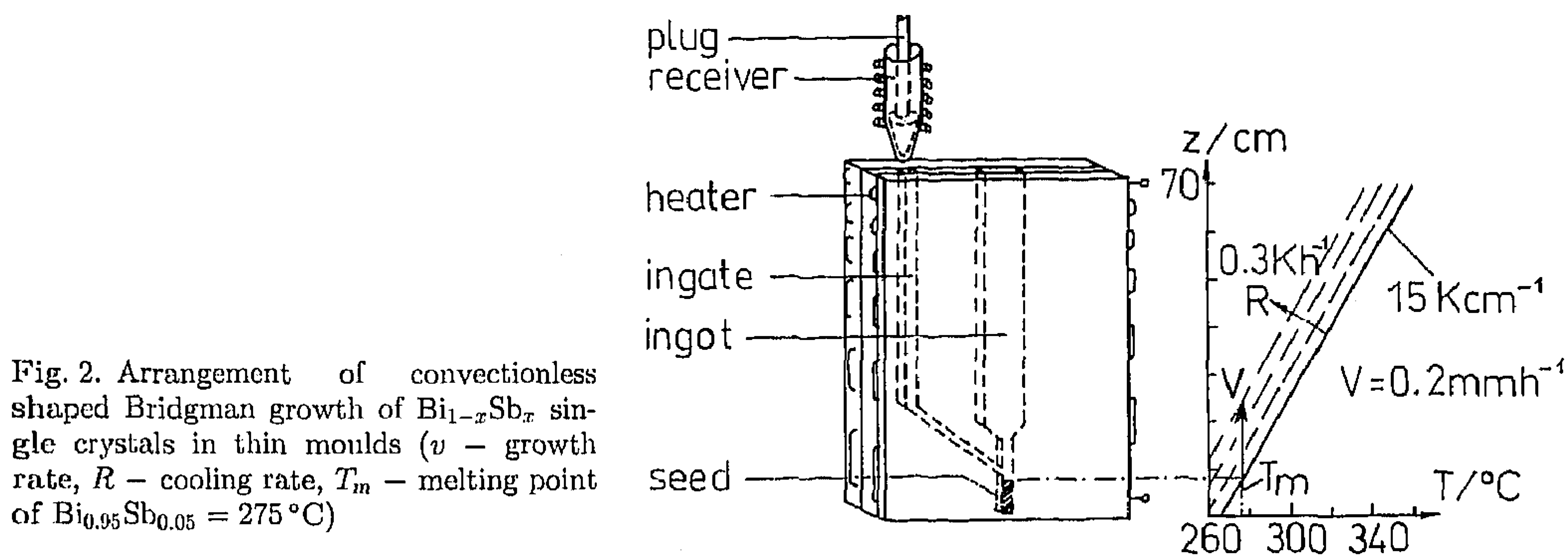


Fig. 2. Arrangement of convectionless shaped Bridgman growth of $\text{Bi}_{1-x}\text{Sb}_x$ single crystals in thin moulds (v - growth rate, R - cooling rate, T_m - melting point of $\text{Bi}_{0.95}\text{Sb}_{0.05} = 275 \text{ °C}$)

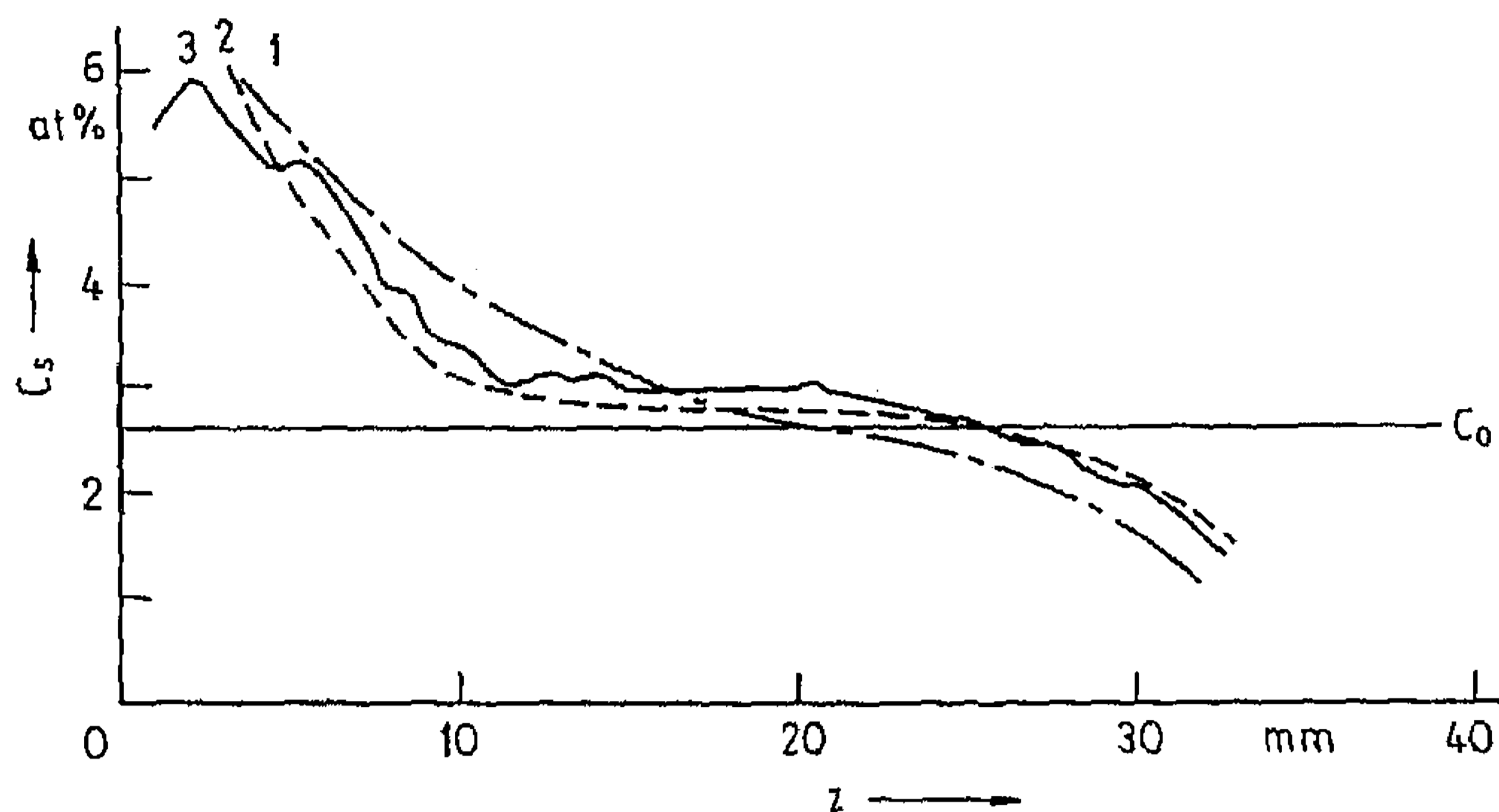


Fig. 3. The axial distribution of Sb in a $\text{Bi}_{0.95}\text{Sb}_{0.05}$ crystal $c_s(z)$ grown under convectionless based ground conditions shown in Figure 2 (1 – theoretical segregation curve acc. to SMITH et al. without consideration of the thermodiffusion, 2 – theoretical distribution corrected by thermodiffusion, 3 – experimental segregation curve measured by EPMA)

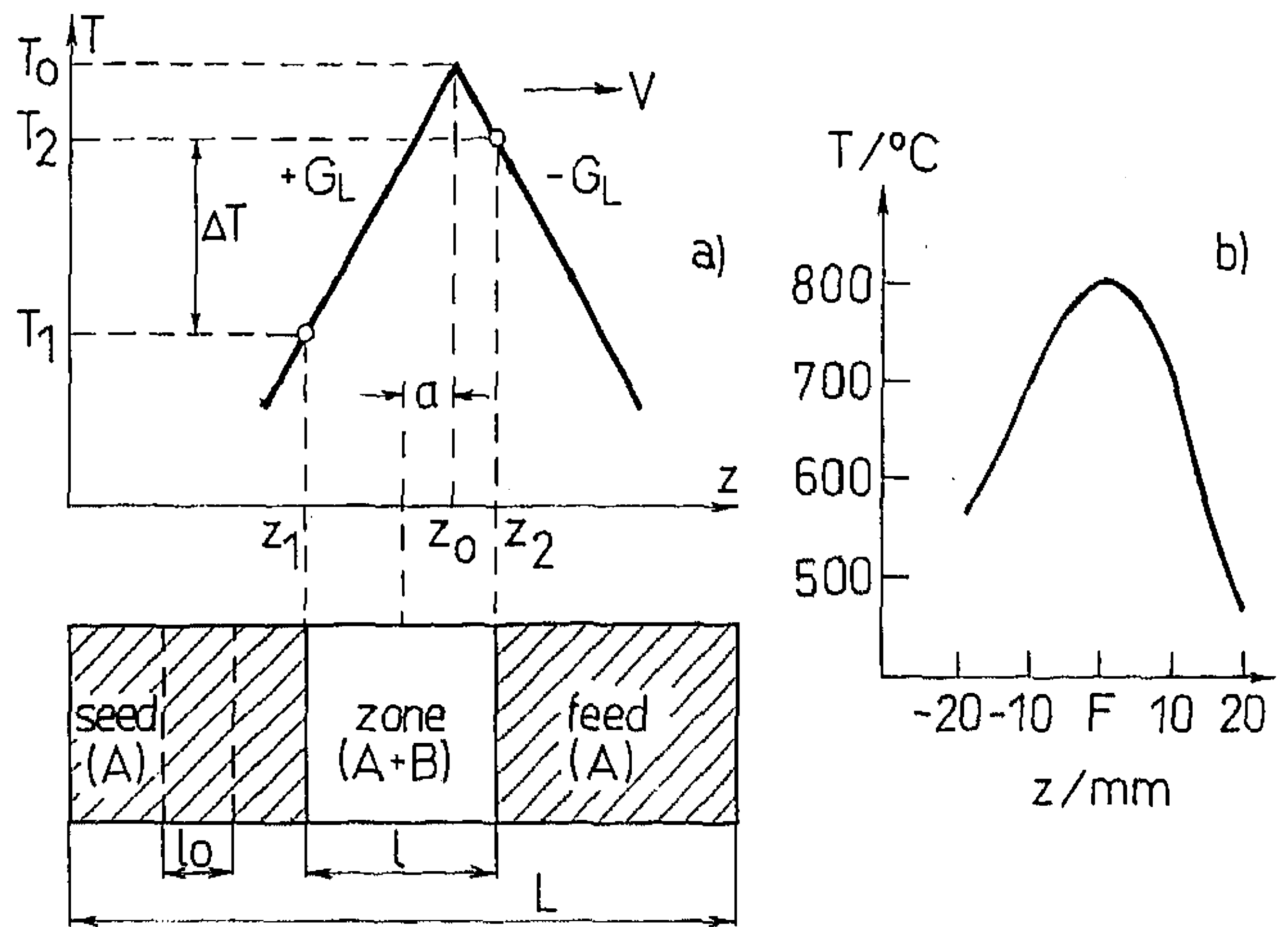
with an accuracy of $\Delta x = \pm 10^{-4}$ (curve 3) in comparison with the theoretical estimated distribution from SMITH et al. (curve 1) and our calculations considering the Soret effect (curve 2), assuming a segregation coefficient of $k_0 = 2.5$. The effect of thermodiffusion was taken into consideration using a combination of the distribution function of SMITH et al. and the formula for Soret separation effect in mixed melts acc. to DE GROOT. A detailed mathematical derivation is given by SCHMIDT. Using $S_T = 4 \times 10^{-3} \text{ K}^{-1}$ a thermodiffusion-driven decomposition over the starting length of the $\text{Bi}_{0.975}\text{Sb}_{0.025}$ melt of about 13% with enrichment of Bi atoms at the growing interface (at the bottom of the ingot) has been approximated. The better agreement of the experimentally obtained profile with curve 2 is obvious.

Settling of the heavier Bi atoms can be neglected since the gravity-driven decomposition force $(m_{\text{Bi}} - m_{\text{Sb}})gl$ is several orders of magnitude smaller than the kinetic mixing energy kT of dissimilar atoms (SCHMIDT), with m_{Bi} , m_{Sb} the mass of Bi and Sb, g the gravitational acceleration, l the length of the melt column parallel to g , k the Boltzmann constant and T the absolute temperature. In fact, taking $l = 50 \text{ mm}$ (Fig. 2) and $m_{\text{Bi}} - m_{\text{Sb}} = 1.45 \times 10^{-25} \text{ kg}$ the relation $(m_{\text{Bi}} - m_{\text{Sb}})gl/kT$ becomes only 9×10^{-6} . The results of former μg crystal growth experiments on board of "Salut 6" with the same material system (SCHNEIDER et al.) may indicate an equal effect. It can be concluded from Figure 3 that the effect of Soret in convectionless Bi–Sb melts leads to an elongated region of axial homogeneity in the crystals in comparison with the distribution function of normal freezing without consideration of thermodiffusion. Further experiments under microgravity should take this important fact into consideration.

3. The travelling heater method (THM)

The THM has proved successful in growing of single crystals which are difficult to produce by conventional techniques (TRIBOULET). A melt-solution zone moves with a constant velocity, beginning at a seed crystal, through a polycrystalline feed ingot. This method is very popular in μg investigations because of drastically reduced growth temperatures, equilibrium pressures, thermomechanical stress forces, and the absence of Marangoni convection. In most cases, a mirror heating facility is applied (EVER et al.) and is capable of producing temperature gradients of $\geq 100 \text{ K cm}^{-1}$ within the liquid zone (KOTTLER, LANGBEIN; TRESER et al.). The principal scheme of the THM is shown in Figure 4a with respective mirror heating temperature distribution (Fig. 4b). Thus, to establish a triangular approximation of the temperature field within this zone (Fig. 4a). A steep temperature distribution with a marked maximum in the multicomponent liquid

Fig. 4. Schematic principle of the THM growth system (a) and a typical mirror heated temperature distribution (b) acc. to EYER et al. (T – temperature, z – distance, G_L – temperature gradient in the liquid zone, l – zone length, l_0 – initial length of zone, T_1, T_2, T_0 – temperatures corresponding to z_1, z_2, z_3, a – asymmetry, v – heater velocity)



requires an examination of the thermodiffusive mass transfer contribution during the growth run in a microgravity environment.

We have theoretically analysed the influence of thermodiffusion on the mass distribution within the THM melt-solution zone of the semiconductor systems IV–VI (PbTe), III–V (GaAs, InP) and II–VI (CdTe). The physicochemical parameters are taken from Table 1 and phase diagrams. Whereas the IV–VI and II–VI liquids were treated as associated melt-solutions (JORDAN) consisting of PbTe and CdTe molecules and Te solvent atoms, the III–V compounds were assumed to be dissociated (the amount of associated complexes is relatively small (see OSAMURA and MURAKAMI) consisting of unpaired separate atoms of Ga, As and In, P, respectively).

We solved a system of, linear phenomenological equations with free boundary value problem for the only independent diffusion flux j_B , without consideration of Dufour effect. Details of the mathematical analysis are given by BOECK, and BOECK, RUDOLPH. Only the final formulas important for practical consideration are presented.

The zone length can be written as

$$l = \frac{T_S - T_0}{G_L} \frac{1}{D_0 m / 2D + 1} + \sqrt{\left(\frac{T_S - T_0}{G_L} \frac{1}{D_0 m / 2D + 1}\right)^2 + \frac{1}{D_0 m / 2D + 1} \left(\frac{2l_0 m}{G_L} + \frac{D_0 m}{2D} 4a^2\right)} \quad (3)$$

with the geometrical parameters given in Figure 4.

The asymmetry (difference in location between the middle of the zone and temperature maximum during the movements of the heater) is given as

$$a = \frac{1}{2} \frac{v m l_0}{D G_L (D_0 m / D + 1)} \quad (4)$$

The temperatures and concentrations at the phase boundaries are taken as

$$T_1 = T_0 + G_L (z_1 - z_0) = T_S - m c_{B1} \quad (5)$$

$$T_2 = T_0 - G_L (z_2 - z_0) = T_S - m c_{B2} \quad (6)$$

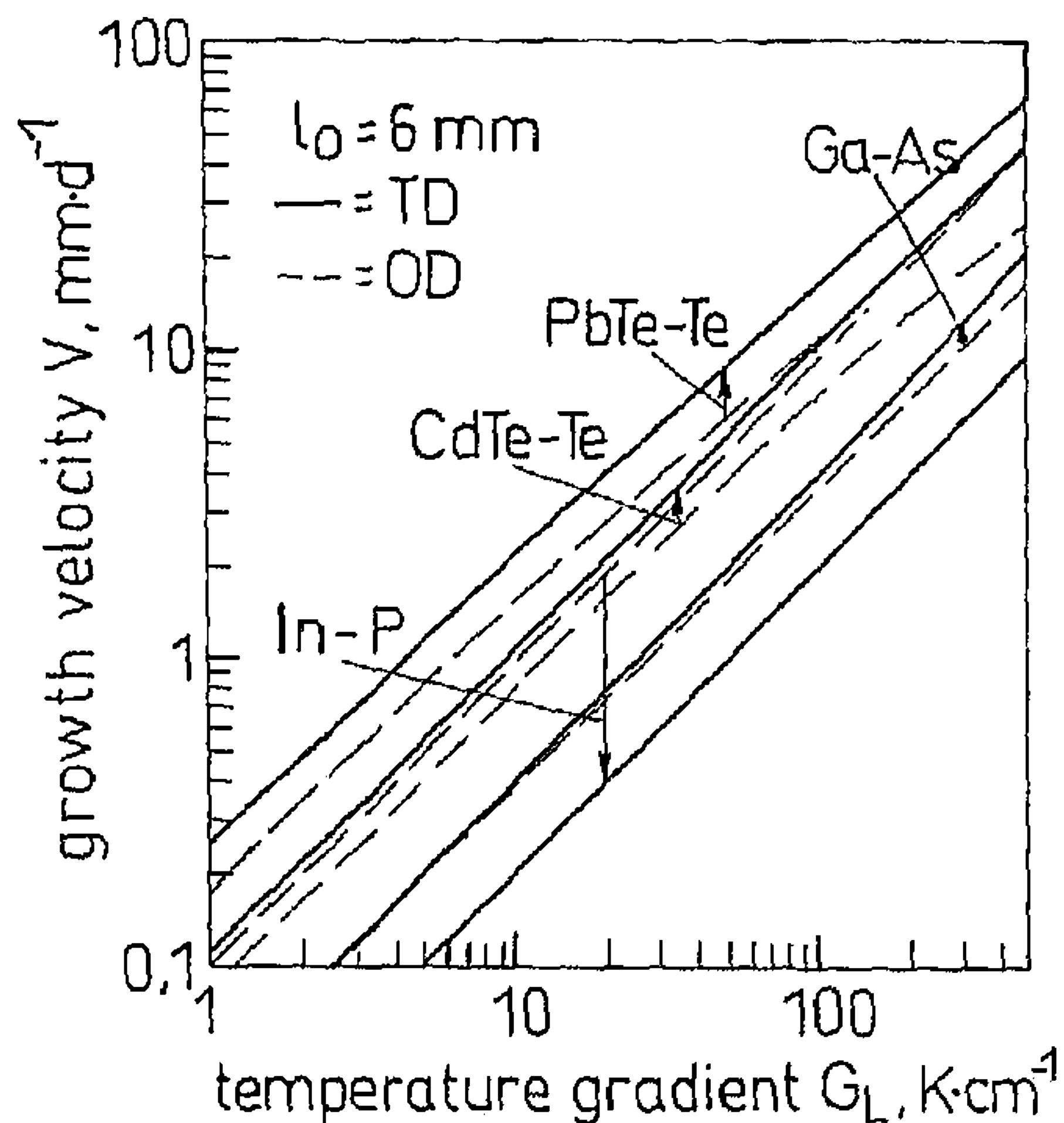


Fig. 5. Theoretical estimated maximum THM heater velocity vs temperature gradient for convectionless crystal growth of various semiconductors under consideration of thermodiffusion TD (heavy lines) and without thermodiffusion OD (broken lines)

with m the slope of liquids in the phase diagram. Finally, the maximum heater velocity $v = v_{\max}$ is found when $a = l/2$ and

$$v_{\max} = D \left\{ - \frac{(D_0 m / D + 1) + (T_s - T_0)}{m l_0} + \sqrt{\left[\frac{(D_0 m / D + 1) (T_s - T_0)}{m l_0} \right]^2 + 2 \frac{(D_0 m / D + 1)^2 G_L}{m l_0}} \right\} \quad (7)$$

the value of which is equated with the moment of “zones loss” of the heater.

The results of our calculations are given in Figure 5 and 6. Figure 5 shows the maximum growth velocity $v = v_{\max}$, calculated from equation (7), versus temperature gradient G_L in front of the growing interface at z_1 (see Fig. 4) with and without consideration of thermodiffusion. In the case of PbTe-Te and CdTe-Te the value of v increases

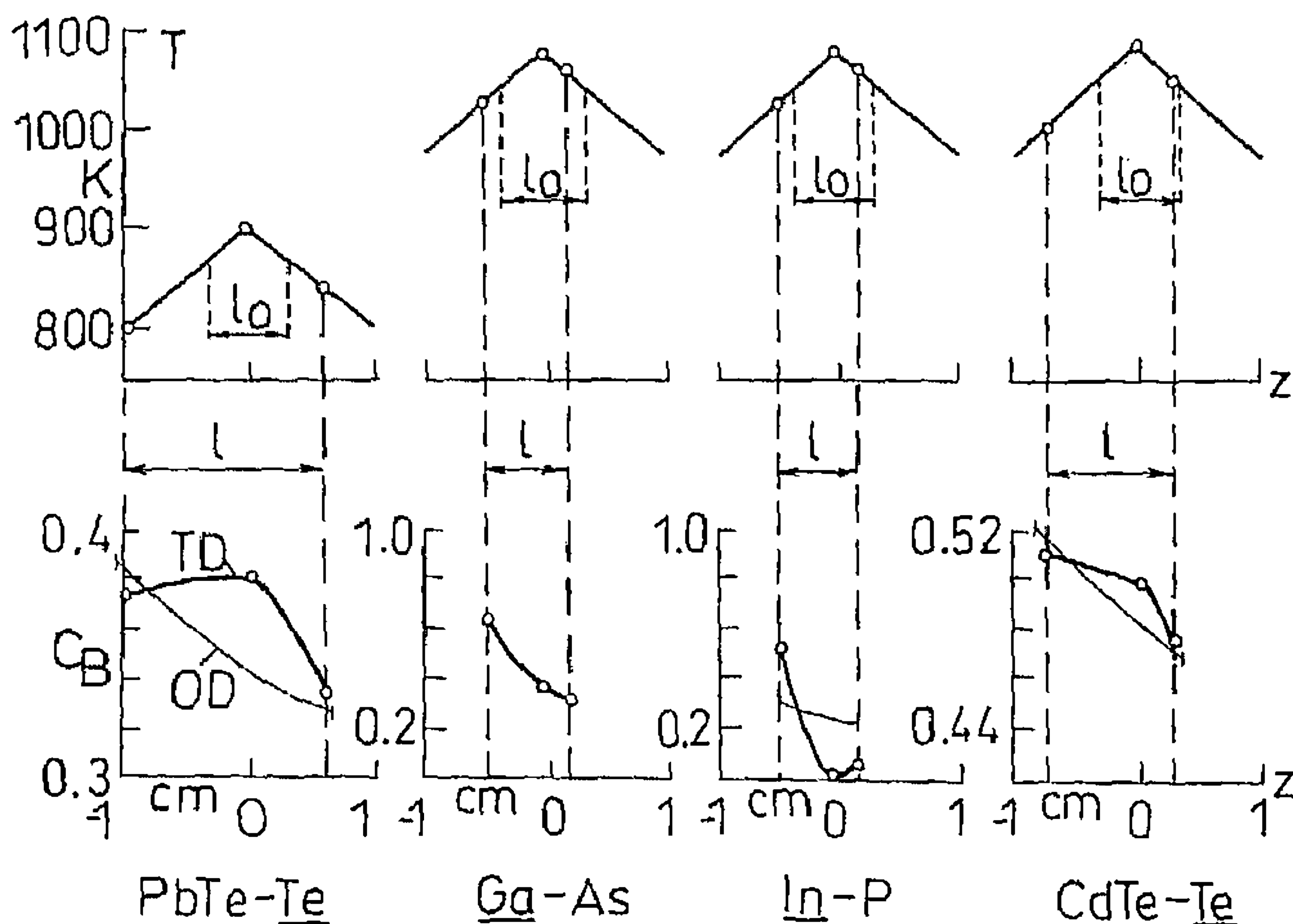


Fig. 6. The distribution of the solvent concentration c_B within the THM zone considering thermal diffusion TD (heavy lines) and when confining the model to ordinary diffusion OD (thin lines) of various material systems with heater velocities 4 mm d^{-1} (PbTe-Te), 2 mm d^{-1} (GaAs-Ga), 1 mm d^{-1} (InP-In) and 4 mm d^{-1} (CdTe-Te)

drastically on account of the Soret effect, which is advantageous for reducing the experiment time under spacelab conditions. On the other hand, for the system In–P a reduction of v is predicted. In the case of Ga–As the Soret coefficient seems negligible.

Figure 6 shows the expected solvent distributions within the THM zone under μg conditions for given temperature fields. We have calculated the concentration fields with (TD) and without (OD) consideration of thermodiffusion for $v > 0$ (moving heater), whereas the velocities used are taken from calculated optimum conditions for each material system. As can be seen the Soret effect is predicted to cause an enrichment of tellurium in the middle of the zone in the cases of PbTe and CdTe. On the other hand the growth of InP is characterized by an enrichment of the solvent In at the growing interface which leads to morphological destabilizing (see next section). In the system GaAs a thermodiffusive effect should be negligible.

4. Morphological stability

As well known, the morphological stability requires growth conditions which avoid a constitutional supercooling at the front of the growing interface. Given the concentration field in the melt-solution due to the thermodiffusive mass transfer, the estimation of the critical growth velocity v_{cr} gives

$$v_{cr} \leq \frac{DG_L/m + D_0G_L}{c_{BL} - c_{BS}} \quad (8)$$

where c_{BL} and c_{BS} are the solvent concentrations in the liquid directly at the interface (z_1) and in the solid ($c_{BS} = k_0c_{BL}$), respectively.

Some important practical consequences for the above mentioned semiconductor systems are shown in Figure 7. In the case of an actual temperature gradient G_L of 100 K cm^{-1} , PbTe crystals grow stable up to 8 mm d^{-1} in comparison with ordinary diffusion which limits the stable crystallization rate to about 4 mm d^{-1} . In other words, thermodiffusion increases the morphological stability. An opposite effect will occur in the case of InP growth where the Soret effect destabilizes growth. Therefore, the enrichment of the solvent In at the front of the interface limits the growth velocity to about 1 mm d^{-1} .

Note, the results of InP are based on the quite hypothetically assumption that the melt-solution is completely dissociated and a negative Soret coefficient takes places

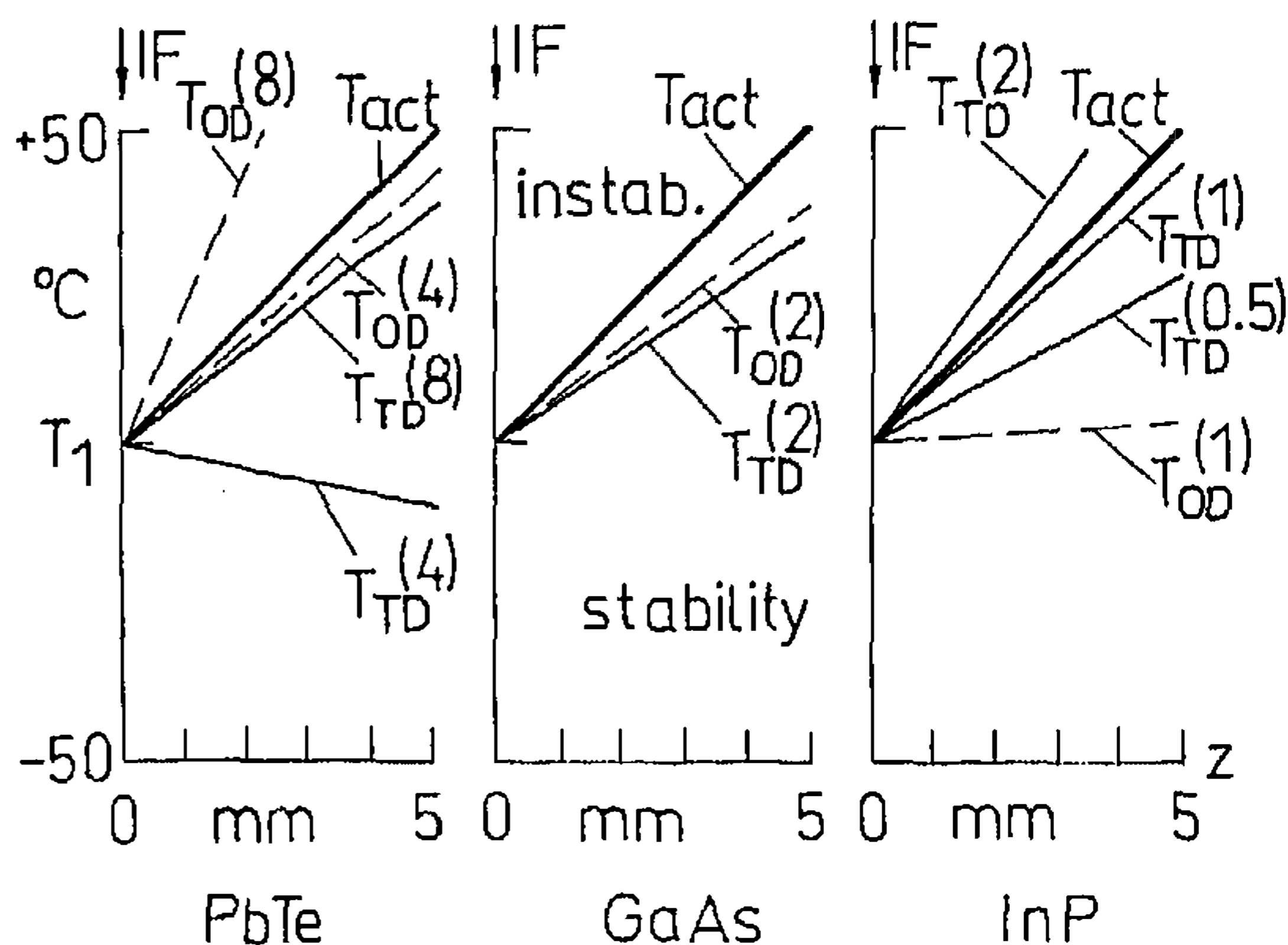


Fig. 7. The distribution of the actual temperature T_{act} at the interface IF ($G_L = 100 \text{ K cm}^{-1}$) and the equilibrium temperatures in the cases of thermodiffusion T_{TD} and ordinary diffusion T_{OD} at various heater velocities (given in mm d^{-1} in the parentheses)

(CHIEN, MATTES; see Tab. 1). However, it is well known (OSAMURA, MURAKAMI) that, in reality, the relatively high ionicity of InP causes a partially associated melt consisting species of InP molecules (solute) and In atoms (solvent). For such a case, of course, the Soret coefficient from Table 1 needs to be revised and a thermodiffusive flow of the heavier InP molecules to the cold crystallization front should to be taken in account. In fact, recently DANILEWSKY and BENZ obtained at first μg THM experiments with InP during D1-mission a markedly increase of the critical growth velocity for the onset of morphological instability at the interface that contradicts our theoretical considerations. Moreover, they found an increased effective diffusion coefficient (i.e. kinetic crystallization velocity) compared to the 1g experiment that may give the important hint on the existence of InP species which under μg conditions are enriched at the growing interface by the effect of thermodiffusion. Well designed further space experiments should be carried out to accurately analyse this phenomenon of InP:In growth. In general, more μg investigations of the effect of thermodiffusion in melt-solutions of semiconductor compounds are necessary in order to test our theoretical estimations.

5. Conclusions

Crystal growth experiments of multicomponent systems without natural and surface tension-driven convection under μg conditions require an exact analysis of the total diffusion flux with consideration of the Soret effect in the liquid phase. The greater the mass difference between the solute atoms or molecules ("crystal building blocks") and the solvent atoms, the higher the Soret coefficient leading to destabilizing or stabilizing of the growth conditions. In convectionless modified Bridgman growth arrangements of $\text{Bi}_{1-x}\text{Sb}_x$ mixed crystals the thermodiffusion helps to increase the axial extension of the homogeneous distribution region of the concentration profile in normal freezing.

It has been shown from theoretical point of view that in THM growth configurations an enrichment ($S_T < 0$) or impoverishment ($S_T > 0$) of the solvent at the interface within the liquid zone will be obtained. Therefore, in the case of CdTe:Te and PbTe:Te the critical growth velocity can be increased drastically under μg conditions. Conversely the THM growth of InP single crystals from In-rich solutions needs a reduced crystallization rate. In the system GaAs:Ga the Soret effect may be ignored. Identical predictions are valid for the critical growth parameters of PbTe, CdTe, InP, and GaAs in order to avoid morphological instabilities.

Recently published results on THM experiments under microgravity gave the hint on the possible existence of associated InP species in the melt-solutions that contradicts our preconditions and requires the revision of the Soret coefficient. Thus, further space experiments are of importance for the practical test of the presented theoretical calculations i.e. Soret coefficients.

This work was supported by the Volkswagen Stiftung under contract number 1/65988.

References

- BOECK, T.: PhD Thesis, Humboldt-Universität zu Berlin 1989
- BOECK, T., RUDOLPH, P.: J. Cryst. Growth **79** (1986) 105
- CHIEN, C. P., MATTES, B. L.: J. Vac. Sci. Technol. **B1** (1983) 648
- CHRIST, B., OELGART, G., STEGMANN, R.: phys. stat. sol. (a) **71** (1982) 463
- DANILEWSKI, A. N.: PhD Thesis, Albert-Ludwig-Universität, Freiburg 1991

- DANILEWSKI, A. N., BENZ, K. W.: J. Cryst. Growth 97 (1989) 571
DISMUKES, J. P., YIM, W. M.: J. Cryst. Growth 22 (1974) 287
EYER, A., NITSCHKE, R., ZIMMERMANN, H.: J. Cryst. Growth 47 (1979) 219
FEUERBACHER, B., HAMACHER, H., NAUMANN, R. J. (eds): Material Science in Space, A Contribution to the Scientific Basis of Space Processing, Springer, Heidelberg 1986
DE GROOT, S. R.: Physica 9 (1942) 699 (see also thesis, University of Amsterdam 1942)
JORDAN, A. S.: Metallurgical Transactions 1 (1970) 239
KOTTLER, W., LANGBEIN, D.: BMFT, Forschungsbericht W 82-018, Bonn 1982
NACHTRIEB, N. H.: Selfdiffusion in Liquid Metals, ins: Int. Conf. on Properties of Liquid Metals, eds Adams, Davie, Epstein, Taylor and Francies, London 1967
OSAMURA, K., MURAKAMI, Y.: J. Phys. Chem. Solids 36 (1976) 931
ROSENBERGER, F.: Fundamentals of Crystal Growth, Springer, Heidelberg 1979, pp. 244 ff.
RUDOLPH, P.: Profilzüchtung von Einkristallen, Akademie Verlag, Berlin 1982
SCHMIDT, P.: PhD Thesis, Humboldt-Universität zu Berlin 1979
SCHNEIDER, G., HERRMANN, R., KRÜGER, H., RUDOLPH, P., KUHL, R., RÖSTEL, R.: Cryst. Res. Technol. 18 (1983) 1213
SMITH, V. G., TILLER, W. A., RUTTER, J. W.: Canad. J. Phys. 33 (1956) 723
SORET, Ch.: Arch. Geneve 3 (1979) 48
TRESER, E., LEXOW, B., KRÄMER, V.: DARA Symposium 1991, Forschung unter Weltraumbedingungen, RWTH Aachen 1991, p. 320
TRIBOULET, R.: Progr. Crystal Growth and Charact. 28 (1994) 85
WINTER, F. R., DRICKAMER, H. G.: J. Phys. Chem. 59 (1959) 1229

(Received, accepted September 13, 1995)

Authors' addresses:

Prof. Dr. P. RUDOLPH, Dr. T. BOECK
Institut für Kristallzüchtung
Rudower Chaussee 6, 12489 Berlin, Germany

Dr. P. SCHMIDT
University of Nijmegen
Department Experimental and Solid State Physics III
Toernooiveld, 6525 Ed Nijmegen, NL